

THE INFLUENCE OF TEMPERATURE AND MAGNETIC FIELDS  
ON DAMPING CAPACITY IN AN  
EVACUATED ENVIRONMENT

by

DONALD LAVERNE CARTER

B. S., University of Missouri at Rolla, 1965

---

A MASTER'S REPORT

submitted in partial fulfillment of the

requirements for the degree

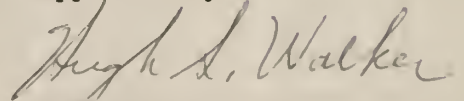
MASTER OF SCIENCE

Department of Mechanical Engineering

KANSAS STATE UNIVERSITY  
Manhattan, Kansas

1967

Approved by:

  
Major Professor

2665  
K1  
1767  
C-333  
1-2

## TABLE OF CONTENTS

Part		Page
	NOMENCLATURE . . . . .	vi
I.	INTRODUCTION . . . . .	1
	Purpose of this Study . . . . .	1
	The Original Concepts . . . . .	1
	Significance of Internal Damping . . . . .	2
	Source of Internal Damping . . . . .	4
	Factors Affecting Damping . . . . .	5
II.	METHODS OF EXPRESSING DAMPING . . . . .	7
	Amplification Factor . . . . .	7
	Equivalent Dashpot Constant . . . . .	7
	Resonant Peak-Width Technique . . . . .	8
	Quality Factor . . . . .	8
	Logarithmic Decrement . . . . .	9
III.	TEST APPARATUS . . . . .	10
	Vacuum System . . . . .	10
	Beam Support . . . . .	10
	Method of Heating Specimen . . . . .	14
	Heat Shielding of Internal Apparatus . . . . .	14
	Deflecting Mechanism . . . . .	17
	Magnetic Field Coil . . . . .	17
	Specimen . . . . .	17
IV.	TEST INSTRUMENTATION . . . . .	18
	Strain and Temperature Sensing Devices . . . . .	18
	Recording Instrumentation . . . . .	18
V.	EXPERIMENTAL PROCEDURES . . . . .	21
VI.	TEST RESULTS . . . . .	23
VII.	CONCLUSIONS AND RECOMMENDATIONS . . . . .	32
VIII.	REFERENCES . . . . .	34

Part	Page
IX. APPENDIX . . . . .	36
A. Equipment List . . . . .	37
B. Calibration Procedure . . . . .	38
C. Determination of Effects of Air Pressure upon Damping . .	40
D. Determination of Magnetic Saturation . . . . .	42
E. Typical Data . . . . .	44
F. Derivation of Logarithmic Decrement . . . . .	46

## LIST OF TABLES

Table	Page
I. Typical Data — Test No. 1 . . . . .	45

## LIST OF FIGURES

Figure	Page
1. Typical Stress-Strain Hysteresis Loop . . . . .	3
2. Schematic Diagram of Test System . . . . .	11
3. Vacuum System . . . . .	12
4. End View of Vacuum Chamber . . . . .	13
5. Field Coil, Heat Shield, Support, and Specimen . . . . .	15
6. Cross Section of Beam Support . . . . .	16
7. Test Instrumentation . . . . .	19
8. Variation of Logarithmic Decrement with Field Current— Shield in place . . . . .	24
9. Variation of Logarithmic Decrement with Temperature, Test No. 1 . . . . .	25
10. Variation of Logarithmic Decrement with Temperature, Test No. 2 . . . . .	26
11. Variation of Logarithmic Decrement with Temperature, Test No. 1 . . . . .	27
12. Variation of Logarithmic Decrement with Temperature, Test No. 2 . . . . .	28

Figure	Page
13. Variation in Temperature between Beam Ends . . . . .	30
14. Variation of Beam Frequency with Temperature . . . . .	31
15. Variation of Stylus Deflection with Stress at Various Temperatures . . . . .	39
16. Variation of Logarithmic Decrement with Chamber Pressure . . . .	41
17. Variation of Logarithmic Decrement with Field Current . . . . .	43
18. Typical Recorder Traces . . . . .	44
19. Free Vibration with Damping . . . . .	47

## NOMENCLATURE

$\sigma$	stress, psi
$\epsilon$	strain, $\mu$ inches/inch
A	amplification factor, resonant, dimensionless
x	amplitude, inches
F	force, pounds
$\omega$	circular frequency, $2\pi f$ , rad./sec
C	dashpot constant, pound-sec/inch
$C_{eq}$	equivalent dashpot constant, pound-sec/inch
Q	quality factor, $1/2\zeta$ , dimensionless
f	frequency, cycles/sec
$\delta$	logarithmic decrement, dimensionless
W	stored energy, inch-pounds/cubic inch
$C_c$	critical damping constant, pound-sec/inch
$\zeta$	damping ratio, $C/C_c$ , dimensionless
e	base of natural logarithm, 2.718... ., dimensionless
k	spring constant, pounds/inch
ln	natural logarithm
m	mass, pounds
n	number of cycles
t	time, sec
$\psi$	specific damping capacity, dimensionless
P	concentrated load, pounds
$\omega_n$	natural frequency (undamped), cycles/sec

$\omega_d$	natural frequency (damped), cycles/sec
$X(t)$	envelope of $x$
$T$	period
$M$	moment, inch-pounds
$I$	moment of inertia, inches <sup>4</sup>
$R$	radius, inches
$D$	diameter, inches



## PART I

### INTRODUCTION

Internal friction or damping capacity is that property of a solid material which results in energy absorption when the material is stressed cyclically. A vibratory system is a good example of this, in which a part, or parts, of the system experience a cyclic stress. If the system is not forced after being set in motion, the free vibrations can be shown to decay or attenuate with time. Thus, the total vibratory energy of the system is decreasing or a part is continually being lost or absorbed in the material due to internal friction.

Purpose of This Study. With the successful launching of the first nuclear powerplant into space, new questions have been asked concerning the properties of the surrounding structures, namely damping. How does the damping characteristics of a structural member change as it is subjected to these hostile environments? High temperatures and magnetic fields usually associated with space reactors may change the design criterion considerably.

The purpose of this study is to demonstrate the change in damping characteristics with a variation of temperature and magnetic field in a vacuum environment for a ferromagnetic material. The temperature range was sufficient to reach the Curie Point of the metal.

The Original Concepts. Measuring material damping has long been a popular



pastime among experimental physicists. In 1784 Coulomb (1)\*, in his "Memoir on Torsion," not only hypothesized internal damping but also undertook experiments which proved that damping was caused by internal losses in the material. The original conception was that damping in solids was analogous to viscous friction in fluids. Kelvin (2) was the first to present this theory, however, his own experiments made in 1865 failed to verify this hypothesis.

The hysteresis phenomenon was presented by Hopkinson and Williams (3) in 1912 which postulated that the loss was due to the non-coincidence of the upward and downward portions of the stress-strain diagram of a material under cyclic loading. The stress-strain diagram for a complete stress cycle thus corresponded to a closed loop as shown in Fig. 1.

In analyzing this further, Föppl (4) assumed that any strain may be considered to be composed of an elastic portion ( $\epsilon_{2e1}$ ) and a plastic portion ( $\epsilon_{2p1}$ ) for the greatest stress  $\sigma_2$ . The plastic portion is then considered the cause of the hysteresis and energy loss. The greater the area of the loop, the greater the damping capacity of the material.

During the past decade, the scientific and engineering interest in internal damping has increased greatly. As a result of these new interests, research in damping continues at an increasingly high level as indicated by recent bibliographic studies (1)(5).

Significance of Internal Damping. The significance of the damping capacity as an engineering property of materials has received widespread recognition in recent years. Wherever vibrational stresses are encountered (as in turbine,

---

\*Numbers in parentheses refer to references in Part VIII. (page 34)

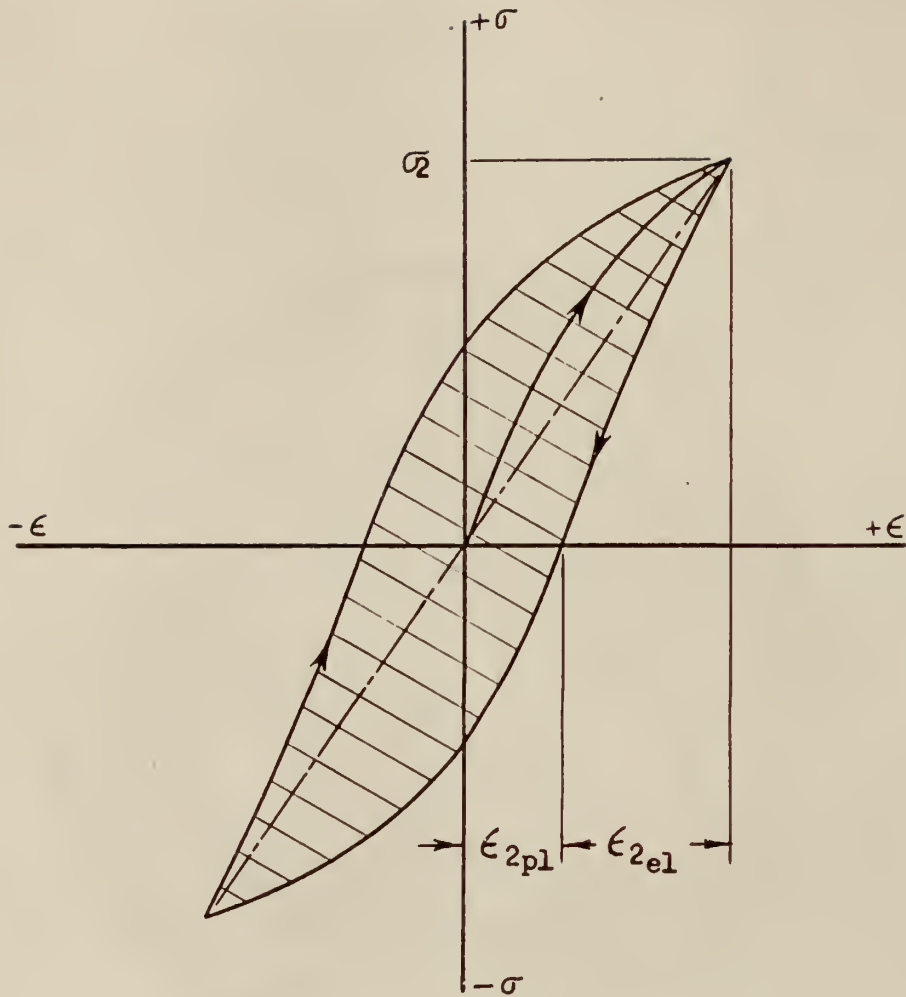


Figure 1. Typical Stress-Strain Hysteresis Loop for a Material Under Cyclic Stress.

compressor, and propeller blades, shafts of various kinds, transmission cables, etc.) the damping capacity of a material may prove to be of more importance than such properties as fatigue strength (4).

Internal damping is, however, not always a desirable property of materials, as might be implied here. It is internal damping which is responsible for the phenomenon of shaft "whirl" (5)(6). Also materials of high internal friction heat up when subjected to vibratory stresses, resulting in a decrease in the strength of the material. Despite the importance of damping capacity as a criterion for the selection of materials for machine and structural parts, relatively little work has been done until recently on damping capacities of engineering materials.

Source of Internal Damping. During the last few decades, the origin of damping in metals has been traced to four sources (7): plastic flow, thermoelastic effect, atomic diffusion, and magnetoelastic effect.

Plastic flow is certainly the most common cause of damping; in high strength alloys, however, plastic flow occurs noticeably only at stress levels beyond those for which the structure is designed. Damping due to the thermoelastic effect becomes noticeable only at a critical frequency whereas the damping attributed to interstitial diffusion of atoms is important only at low stress levels and is also associated with a critical frequency. Consequently, only the magneto-mechanical effect contributes significantly to the large damping capacity in high-strength alloys; and this, of course, is limited to ferromagnetic materials.

The energy dissipated during a stress-strain cycle as a result of the magneto-mechanical effect is generally caused by irreversible magnetostrictive strain. Every ferromagnetic material consists of so-called domains which are

more or less randomly oriented in an unmagnetized material. However, on the application of a magnetic field, or a stress, these domains tend to align themselves in the direction of the field, or in the direction of the tension strain. This movement of the domains then results in an irreversible change of the dimensions of the material which is called "magnetostriction."

Conversely, if such a bar is stretched by a mechanical force, the magnetization of the bar is changed. If the direction of the stress is reversed, the magnetization again changes, so that an alternating stress will cause a continuous change in magnetization and local eddy currents will be produced within the bar which add to the energy loss. A strong magnetic field prevents the mechanical force from changing the magnetization and the eddy current loss is eliminated.

Factors Affecting Damping. In spite of the work being done on the nature of internal friction in solids, there is available no physical theory for this phenomenon, except at the very lowest strains which are out of the range of engineering interest. Seitz (8) has presented a good summary of these in his book.

The factors of importance in regard to internal friction in the engineering range of stresses appears to be as follows: kind of material, stress or strain amplitude, nature of stress or strain, and temperature (9). Several investigations show that frequency has no effect in the range of engineering interest (6)(4).

Very few studies have been conducted to compare the damping in different materials. Hempel (9) does report, in a study of the damping properties of cast irons, that the higher the tensile strength, the lower the damping capacity.



The most important variable affecting internal friction in solids is the stress or strain amplitude of the cyclic action. Hopkinson and Williams (3) were among the first to indicate this stress dependency. The earliest investigators found the energy loss per cycle (damping capacity) to vary about as the fourth power of the stress amplitude. Later investigations, demonstrated by Robertson and Yorgiadis (9), show that the damping capacity varies about as the third power for a considerable range.

As to the effect of the nature of stress involved, there are few data available since most of the experiments have only been performed in torsion. There is evidence that the internal friction under shearing stress is different from that under normal stress (4).

Temperature has been found to have significant effects upon the damping capacity. Measurements by Contractor and Thompson (10) showed that for the steels tested, the damping capacity increased rapidly with increase in temperature for a considerable range. These results compare favorably with those tests reported later in this report.

## PART II

### METHODS OF EXPRESSING DAMPING

Various methods of measuring and expressing damping have been used in the past. Those having some application to engineering needs are discussed briefly here in order to acquaint the reader with methods available.

Almost all descriptions of damping are derived from the linear, single degree of freedom system with viscous damper in parallel with the spring, and so a start of analysis is made from this point of view (11).

Amplification Factor. In a linear, single degree of freedom system, if a constant sinusoidal excitation force is applied with gradually increasing frequency, it will be found that the amplitude of vibration steadily increases to a maximum and then decreases as the frequency is increased. The amplitude reaches a maximum at one value of frequency, at which the driving force is exactly in phase with the vibratory velocity. This amplitude is hence a measure of damping since the applied force is completely dissipated in damping at the resulting amplitude. The ratio between vibration amplitude at resonance and that at zero frequency is therefore a true and dimensionless measure of damping (12) or

$$A = \frac{x_{\text{res}}}{x_{\text{st}}} .$$

Equivalent Dashpot Constant. At resonance, the amplitude of a viscously damped, single degree of freedom system is

$$x_{\text{res}} = \frac{F}{\omega C} .$$

An equivalent dashpot constant can be defined as (13)

$$C_{eq} = \frac{F}{\omega x_{res}}$$

for any damped system, even those which are not viscously damped.

Resonant Peak-Width Technique. With this technique, the frequency of the impressed force is varied through the resonance condition while the energy input is maintained constant. The amplitude of the vibrational response is a maximum when the impressed frequency is equal to the resonant frequency of the specimen and decreases on either side.

If  $\Delta f$  is the change in impressed frequency necessary to change the amplitude of the vibrational response from half-maximum on one side of resonance to half-maximum on the other, then the internal friction at the resonant frequency  $f_0$  is given by (14)

$$Q^{-1} = \frac{\Delta f}{\sqrt{3}f_0} .$$

The bandwidth method is a form of this technique (11). These methods lend themselves readily to experimental measurements where a driving force is used.

Quality Factor. The  $Q$  of a system is defined in terms of the ratio of the energy dissipated to the energy stored. This has been defined as (15)

$$Q = \frac{\pi}{\delta} = \frac{2\pi W}{\Delta W} .$$

Föppl (4) presented his data in much the same way in terms of specific damping capacity. This is defined as the ratio of energy loss per cycle to the vibrational energy of the member

$$\gamma = \frac{\Delta W}{W} .$$



Logarithmic Decrement. Probably the most widely used method of measuring damping, and certainly the one in longest use, is that of measuring the decay rate of torsional pendulum or flexural beam. This method is used in this study since it is the easiest quantity to determine experimentally.

The logarithmic decrement is defined by

$$\delta = \ln \frac{x_n}{x_{n+1}}$$

where  $x_n$  and  $x_{n+1}$  are amplitudes of two successive vibrations. This can be extended as shown in the derivation of the logarithmic decrement in Appendix F to be

$$\delta = \frac{1}{n} \ln \frac{x_0}{x_n}$$

where  $n$  is the number of cycles between  $x_0$  and  $x_n$ .

## PART III

### TEST APPARATUS

A schematic diagram of the entire test system including instrumentation is shown in Fig. 2. Photographs of the apparatus follow in Figs. 3, 4, and 5 to further illustrate the system and its parts. An equipment list has been included also in Appendix A.

Vacuum System. The vacuum chamber was constructed from a twelve inch diameter seamless steel pipe, four feet long. A groove was cut in each end to receive an "O" ring which formed the seal between the steel pipe and a glass plate. Three-fourth inch thick plate glass was used. See Fig. 3.

Sealing the chamber around external connections was done by using one-eighth inch neophreme rubber pressed between the two, flat, mating surfaces. The outside air pressure provided the force to hold the seal. High vacuum grease was used on all mating surfaces.

A Welch vacuum pump was used for evacuating the system. A "U" tube mercury manometer and a Pirani gauge were employed together to measure the higher and lower pressures respectively. The Pirani gauge was used only for pressures lower than 2000 microns. The normal "pump down" time required to evacuate the chamber to a pressure of 1000 microns was 50 minutes.

Beam Support. The cantilever beam support had to meet certain requirements such as rigidity and being electrically and thermally insulated from the specimen. A welded assembly was chosen which was bolted to a permanent base plate within the chamber.

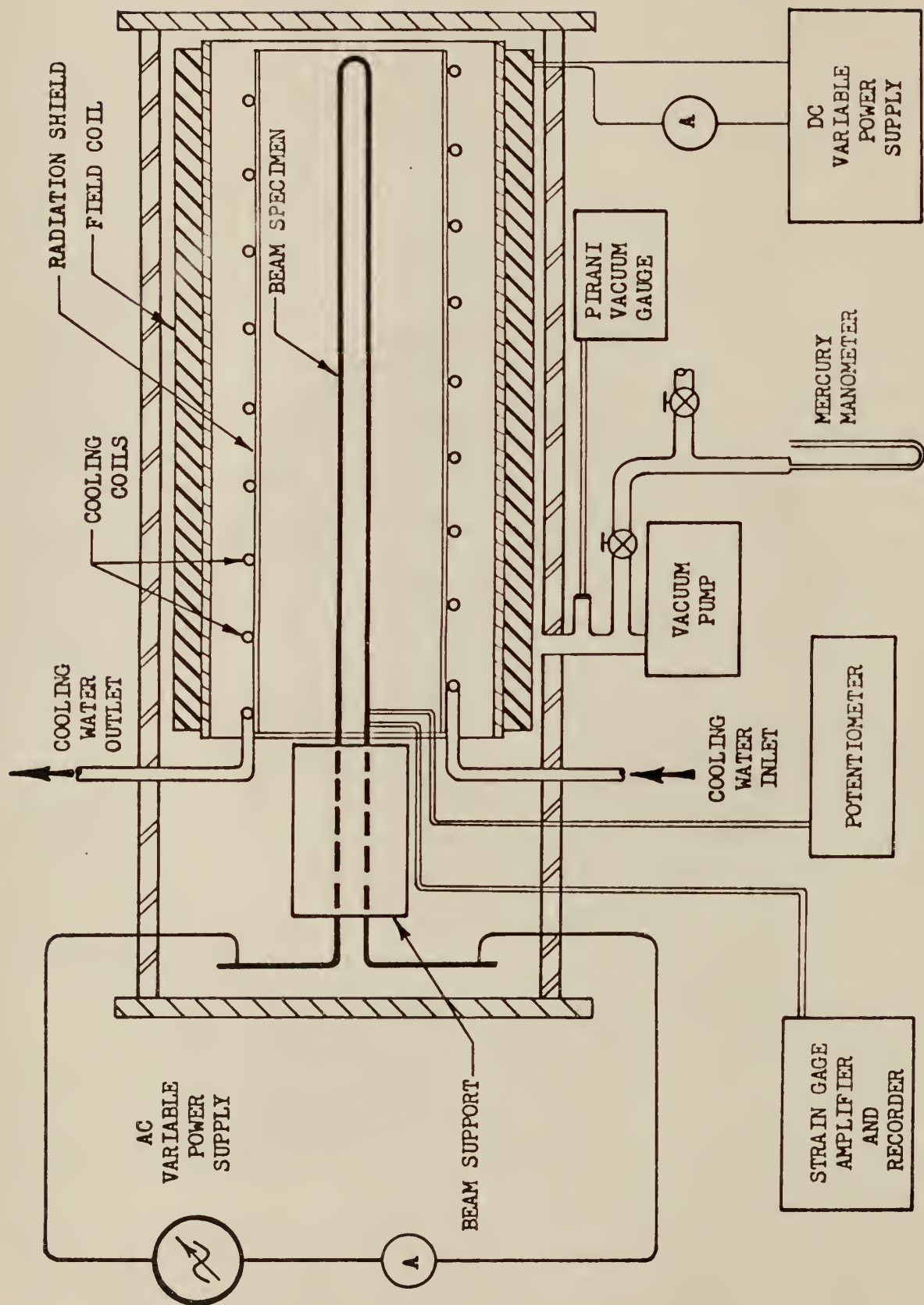


Figure 2. Schematic Diagram of Test System.

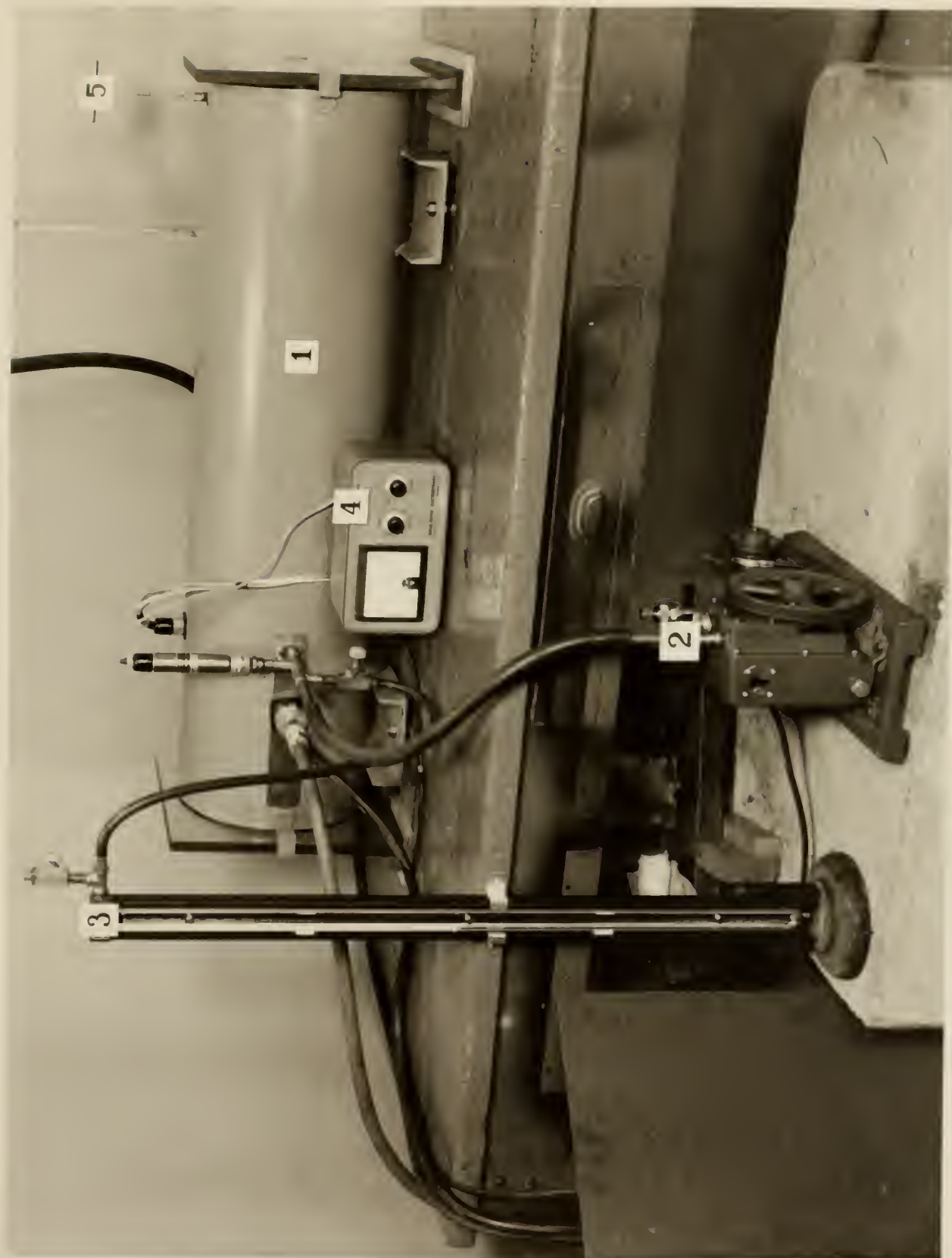


Figure 3. Vacuum System.



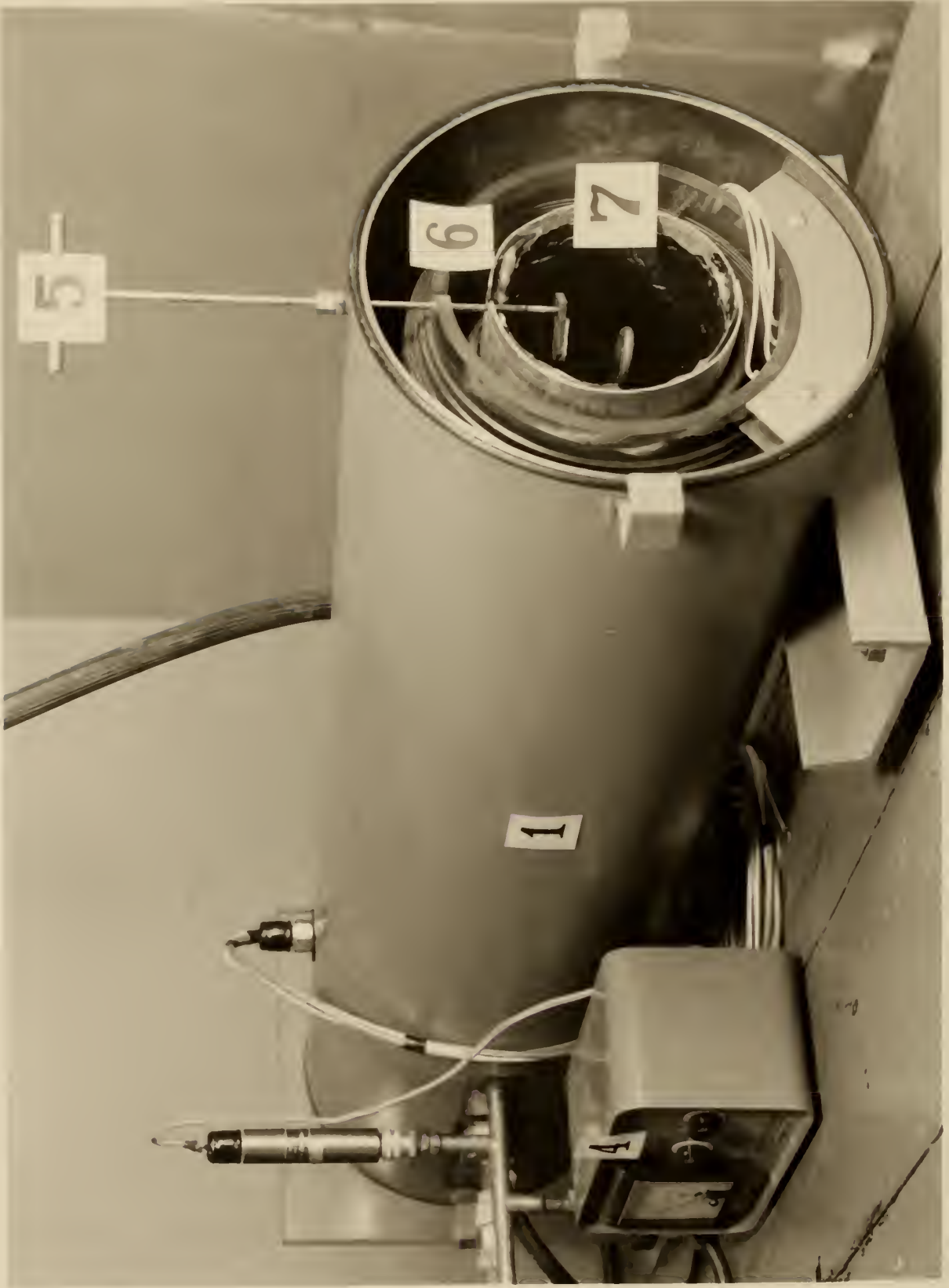


Figure 4. End View of Vacuum Chamber.

One-fourth inch Transite plate was chosen as an acceptable electrical insulator and also for its rigidity. Since Transite is a relatively good thermal conductor, the beam had to be thermally isolated from the support in order to reduce the temperature gradient along the beam. This was accomplished by reducing the conducting surface area. The effective area was actually two intermittent lines rather than a surface. Figs. 5 and 6 best show this arrangement.

Method of Heating Specimen. Electrical resistance heating was used to heat the specimen since this was most convenient to achieve the higher temperatures. This is the reason for the "U" shaped specimen. A welder supplied the necessary AC current to heat the beam.

Heat Shielding of Internal Apparatus. In working with the higher temperatures for long periods of time, much heat was lost by radiation in the evacuated chamber. Since these high temperatures could not be tolerated in the magnetic field coil and the glass ends, a method of shielding and cooling was devised.

A six inch diameter aluminum tube surrounding the entire length of the beam acted as a radiation heat shield. This tube was inside the field coil, concentric with it. The reflectivity of the inner surface was increased further by lining it with aluminum foil. Sheets of foil were also used to shield the glass end of the chamber.

In order to dissipate the heat absorbed by the aluminum, three-eighths inch copper tubing was wound around the outside of the aluminum shield tube for water cooling. This is shown in Fig. 5. The cooling water was fed into and out of the chamber through the brass electrical conductors carrying the AC power to the specimen. This kept the number of chamber openings and seals to a minimum and also eliminated any heat build-up in the power leads within



Figure 5. Field Coil, Heat Shield, Support, and Specimen.



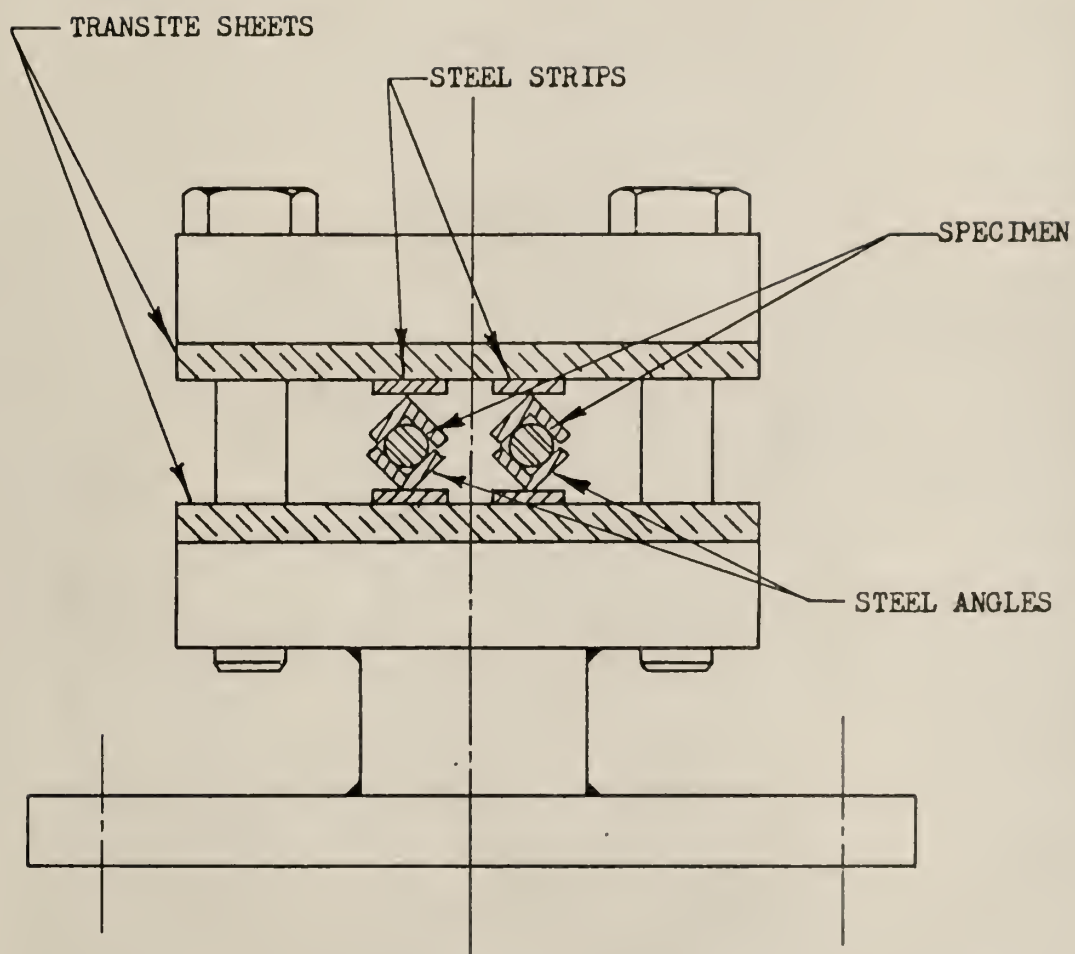


Figure 6. Cross Section of Beam Support

the chamber.

Tests were conducted using the water cooled heat shield and are described later. These tests indicated that the shield adversely affected the results to such an extent that the purpose of this study could not be carried out.

An alternate method of heat shielding was then devised using two layers of aluminum foil inside the plexiglass tube. These layers were separated by a one-fourth inch air gap and placed such as not to make a complete electrical circuit as did the previous shield. This was found to work satisfactorily for periods of two hours, however it could not be used continuously because of eventual heat build-up within the chamber.

Deflecting Mechanism. The mechanism used to deflect the end of the cantilever beam was merely a three-sixteenths inch brass rod extending into the chamber from the top through a brass guide sealed by an "O" ring. The rod was moved up and down and turned manually by the handle on top. See Fig. 4. A "finger" on the other end of the rod displaced and released the beam.

Magnetic Field Coil. The magnetic field was provided by a coil wound with insulated wire on an eight inch diameter plexiglass tube. The length of the coil was sufficient to completely enclose the beam, the center being concentric with the beam center. The coil is shown in Figs. 4 and 5. A variable DC power supply was used to excite the field.

Specimen. The specimen or beam tested was a  $5/16$  inch diameter rod bent into a "U" shape with a  $5/8$  inch radius and an effective length of 34.5 inches. The material was a hot-rolled, mild steel (1020). The reason for the "U" shape was to facilitate heating as mentioned previously.

## PART IV

### TEST INSTRUMENTATION

Strain and Temperature Sensing Devices. Lateral deflections of the cantilever beam were measured by recording the strain at a point just outside the support. This was done so as to not induce additional damping into the system by the lead wires. Since high temperatures were involved in these tests, it was necessary to employ special, high temperature, foil strain gages applied with a ceramic adhesive. These gages were capable of withstanding a sustained temperature of 1500 F.

The temperature of the beam was also monitored just outside the support. A chromel-alumel thermocouple was used, the junction being silver soldered to the beam to provide intimate contact.

Recording Instrumentation. The recording and other instrumentation are pictured in Fig. 7 and shown schematically in Fig. 2. The cyclic strain measurements from the strain gage were permanently recorded on chart paper from the Sanborn Industrial Recorder. Typical output traces are shown in Appendix E. The recorder was coupled with the Sanborn Strain Gage Amplifier. The calibration procedure for these instruments is given in Appendix B.

The potential of the thermocouple or the beam temperature was read out on a millivolt potentiometer with an internal cold reference junction. The temperature was controlled with the variable output welder also shown in Fig. 7. In order to be consistent in varying the temperature of the beam, the high heating current was monitored with a clamp-on ammeter.

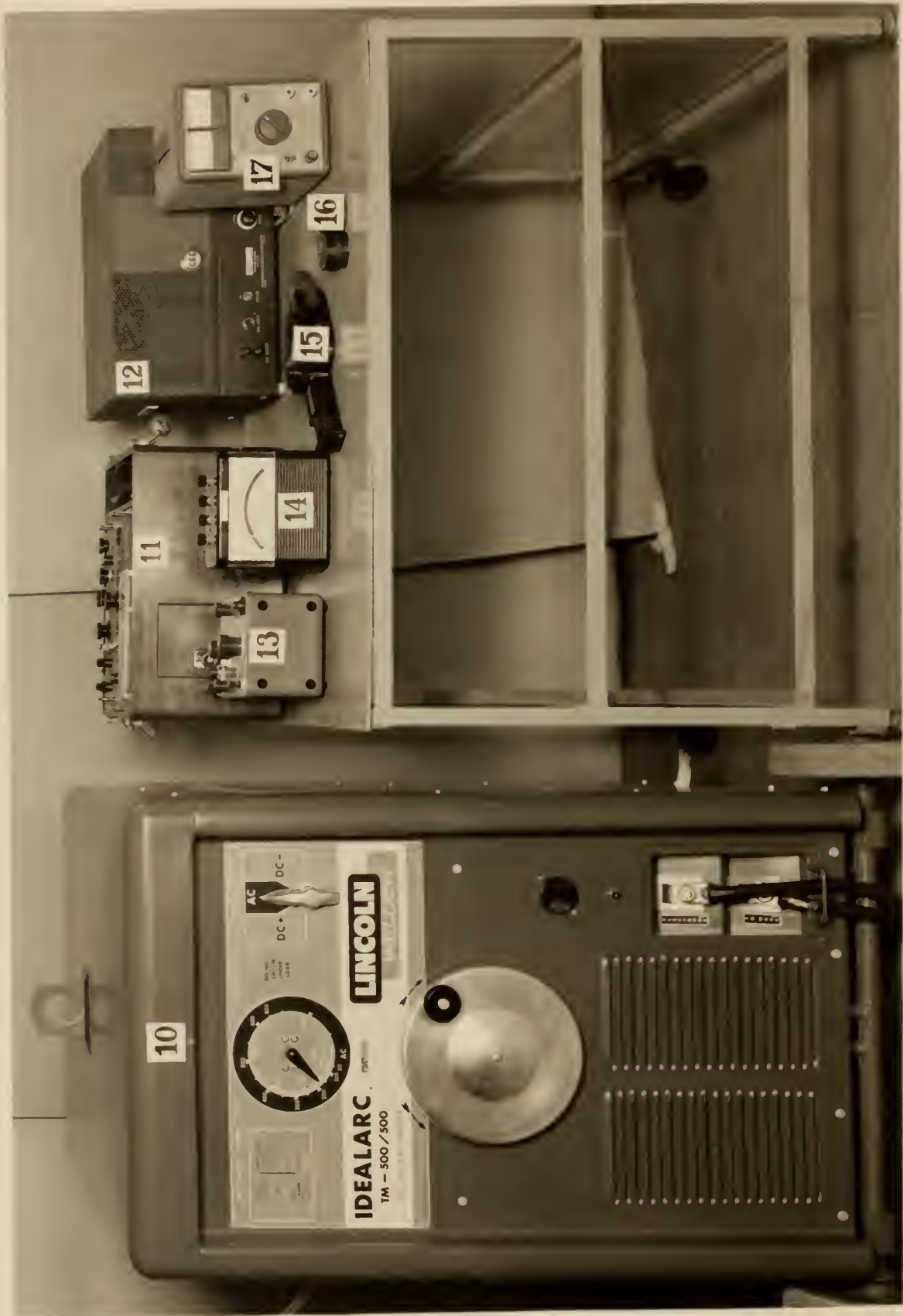


Figure 7. Test Instrumentation.



A DC current to excite the magnetic field was provided by one of two DC power supplies shown. Two power supplies were used since neither of the two provided the total range desired. The field current was measured with a precision ammeter.

## PART V

### EXPERIMENTAL PROCEDURES

The strain gage and recorder were first calibrated to measure stress as a function of recorder deflection for the temperature range to be investigated. See Appendix B. Tests were then conducted to determine the effects of air pressure upon damping and what pressure would be sufficient to render the damping due to air drag insignificant. Appendix C shows these results. Preliminary tests were also conducted to determine the saturation current for the coil to insure that there was a sufficient field strength to align the domains. The saturation curve is shown in Fig. 17, Appendix D.

To set the cantilever beam in motion, the tip of the beam was deflected and released by the mechanism described earlier. A careful attempt was made to deflect and release the beam in exactly the same manner each time. Since the mode shape of a deflected cantilever beam is not exactly that of the natural mode of vibration, the beam was allowed to oscillate and damp into its natural mode before recording any data.

Time and heating current were also recorded at each data point to insure better repeatability of each test. This is shown in a table of typical data in Appendix E. Two recordings were made at each temperature level; one without the magnetic field and one with the field. The strain gage half-bridge was balanced before making each recording.

Since the damping capacity is a function of the stress level, it was necessary to take all data at the same level. A value of 1500 psi was chosen

as a convenient level to work with. As mentioned earlier, the logarithmic decrement was the method used to measure the damping. Since the damping capacity of this particular specimen was quite low, a range of 100 cycles was used in taking measurements for most of the lower temperatures.

It should be noted here that the stress level investigated was always centered in the range of  $n$  cycles, i.e., measurements of  $x_0$  and  $x_n$  were always made at points  $n/2$  cycles on either side of the amplitude corresponding to 1500 psi. This insured a closer average value for the logarithmic decrement. The deflection corresponding to a stress of 1500 psi at each temperature level was obtained from Fig. 15 in Appendix B. Peak to peak amplitudes were used since this was easier to measure and only the ratios were involved in the calculations. The logarithmic decrement was calculated from the equation derived in Appendix F.



## PART VI

### TEST RESULTS

Early testing was conducted using the heat shield and cooling coils described earlier and shown in Fig. 5. After examining the data, it was found that the shield was adversely affecting the magnetic field to such an extent that the purpose of this study could not be carried out.

An attempt to show magnetic saturation was made with the aluminum heat shield in place as pictured in Fig. 4. The results of two of these tests are shown in Fig. 8. Also shown in Fig. 8 is the results of the same test without the shield in place. It was observed that the damping was increased considerably in the presence of a magnetic field with the shield in place; however, it was decreased with the shield removed in the same field. An explanation of this effect was not ventured due to the time available and brevity of this report.

This method of removing heat was eliminated and the tests were continued using foil radiation shields also described earlier. The results of these tests are contained herein.

The test results showed that the presence of a magnetic field does alter the damping characteristics. The logarithmic decrement was decreased measurably and the magnetostrictive damping was shown to be a significant part of the internal damping. This was consistent with the theory presented in the introduction and compares favorably with that work done by Parker (16). This lowering of the damping capacity is readily apparent in Figs. 9 through 12

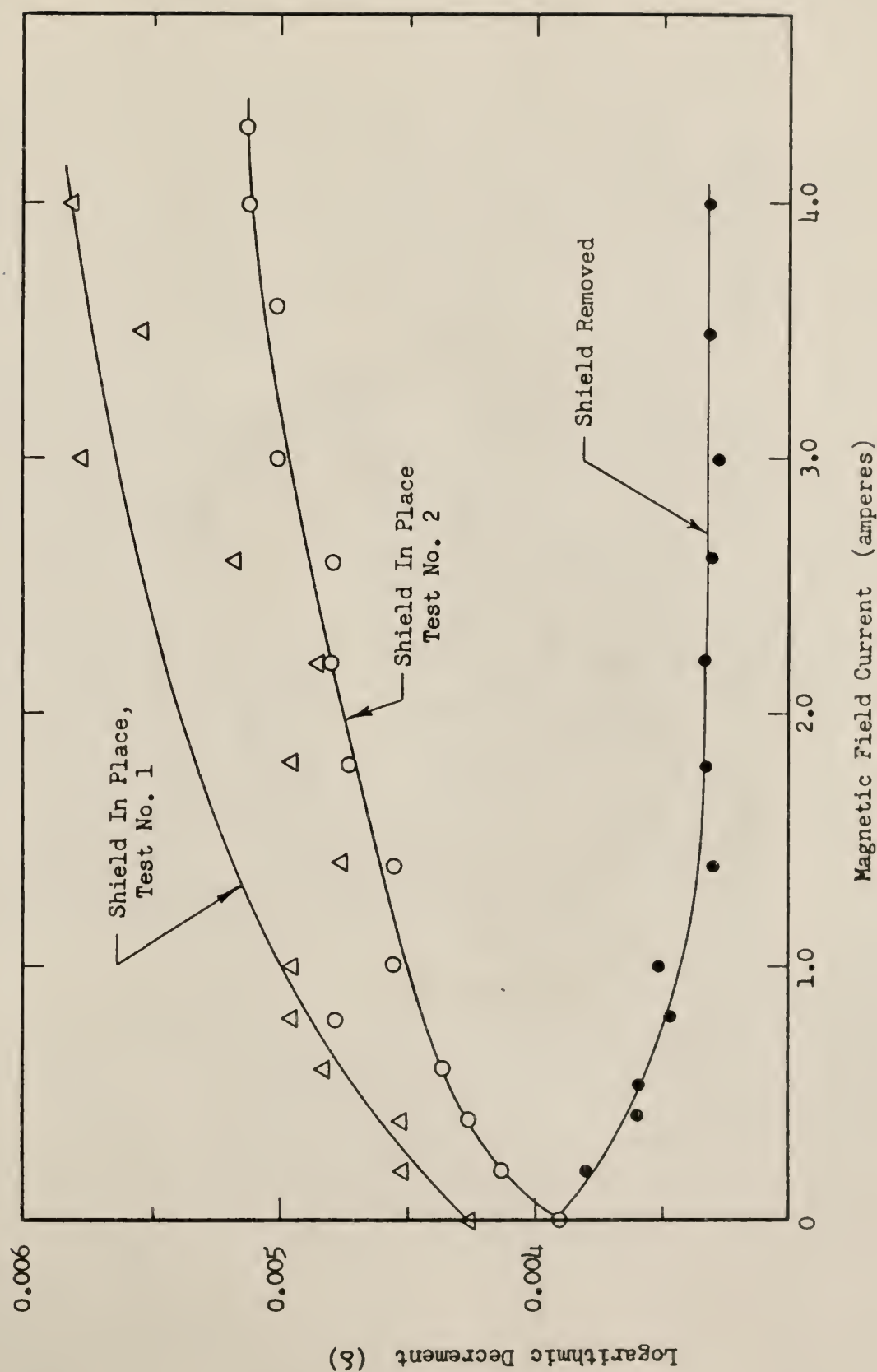


Figure 8. Variation of Logarithmic Decrement with Field Current. Preliminary tests with the aluminum heat shield and cooling coils in place and removed.

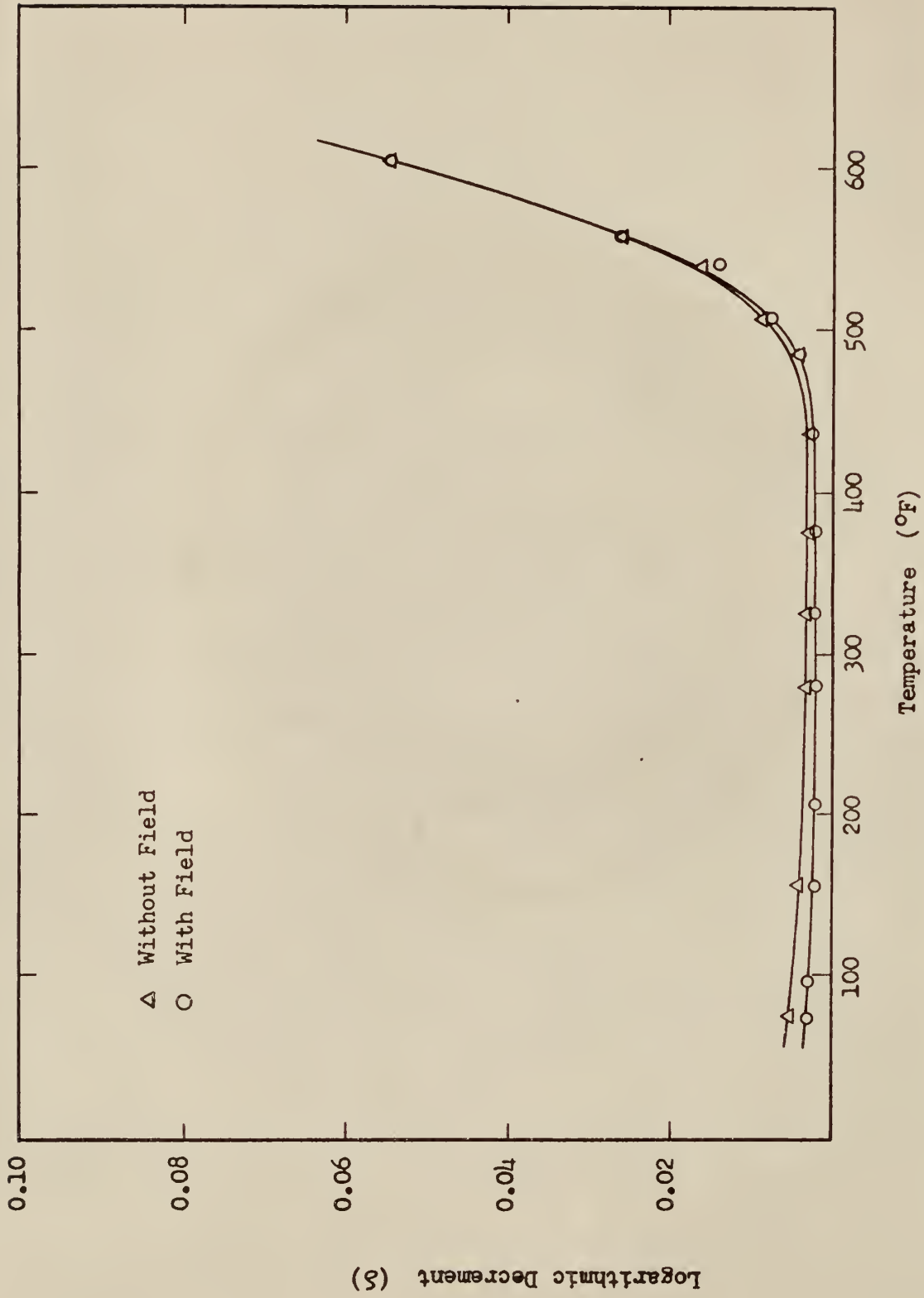


Figure 9. Variation of Logarithmic Decrement with Temperature in an Evacuated Environment, Test No. 1.

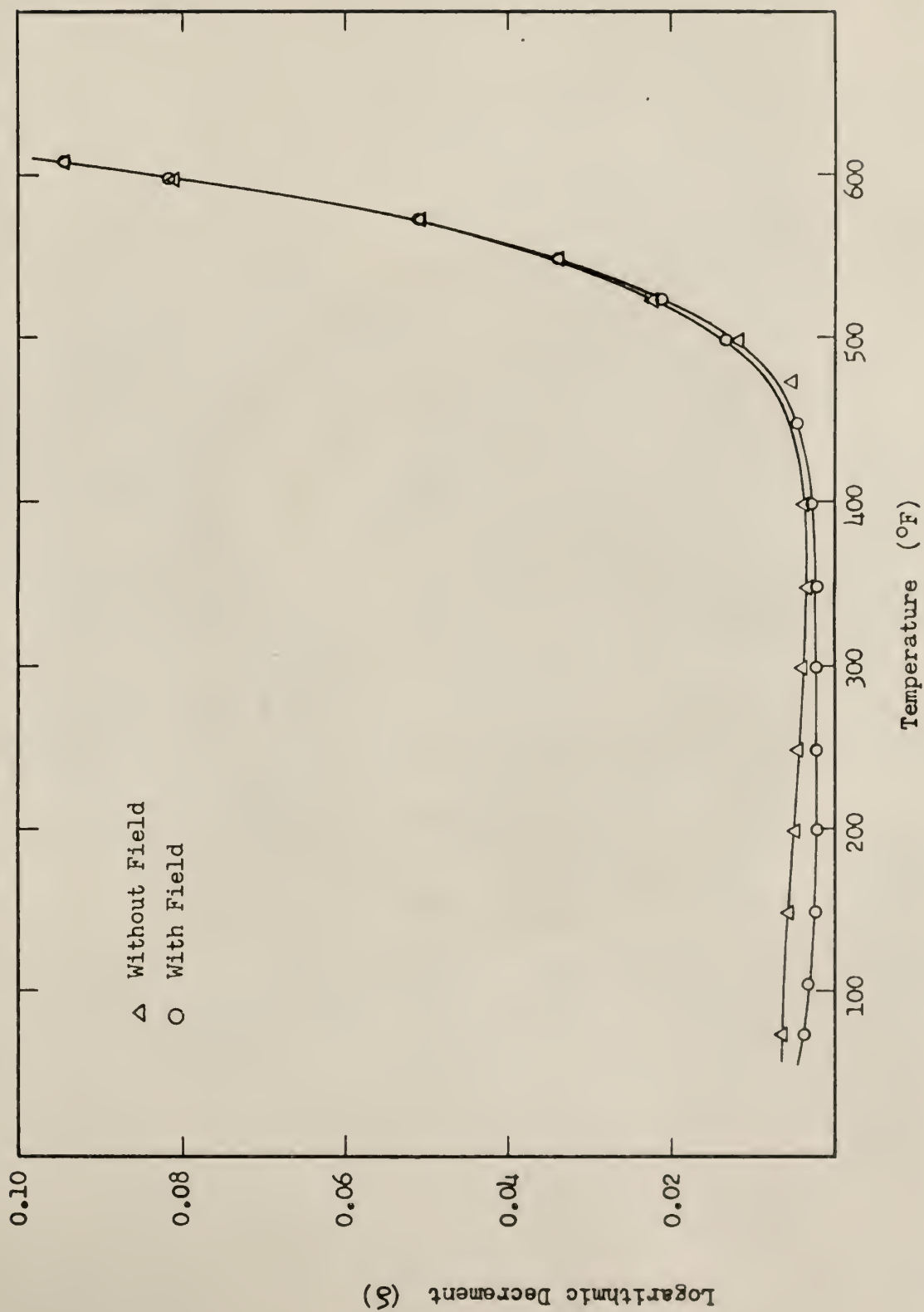


Figure 10. Variation of Logarithmic Decrement with Temperature in an Evacuated Environment, Test No. 2.

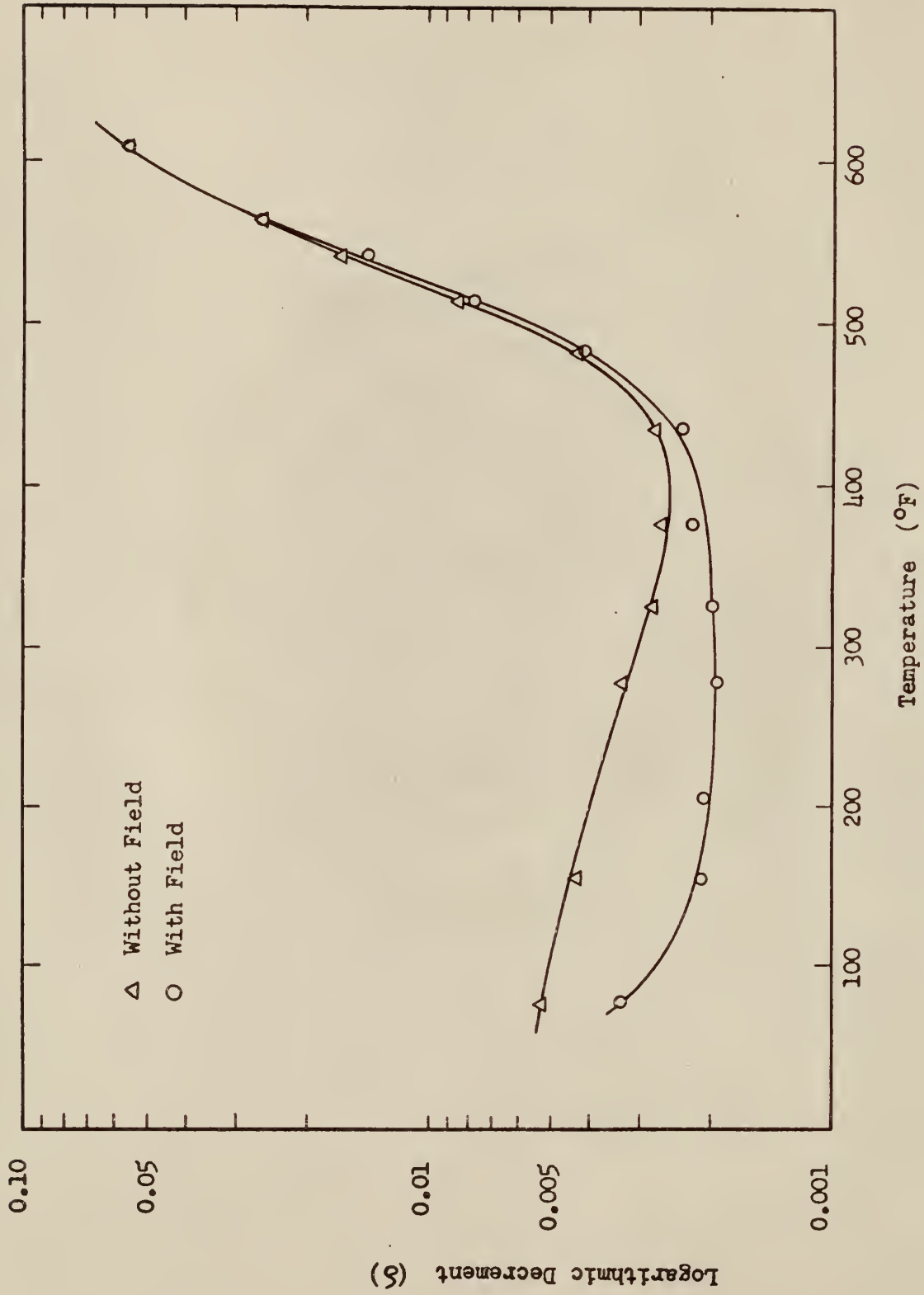


Figure 11. Variation of Logarithmic Decrement with Temperature in an Evacuated Environment, Test No. 1.

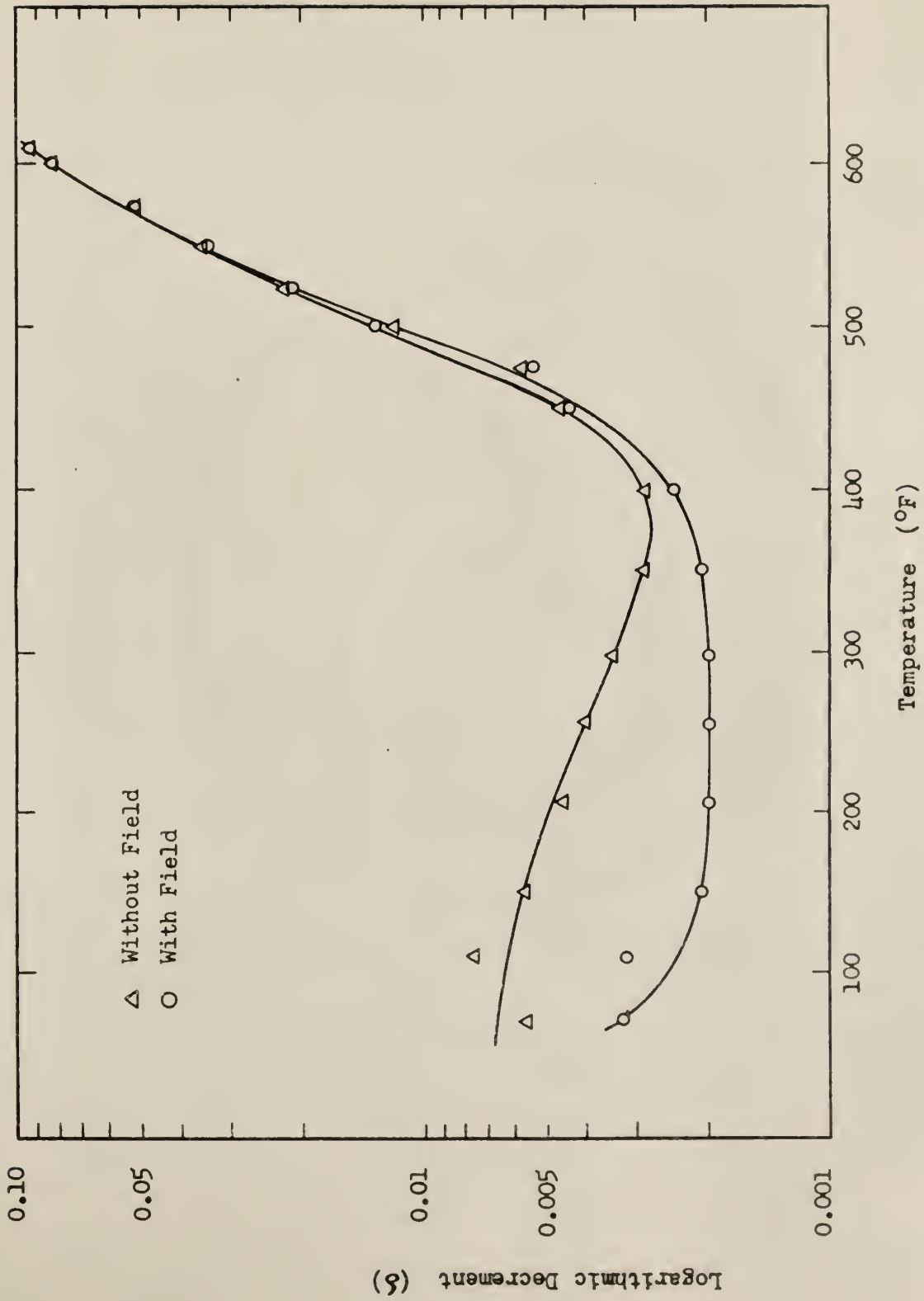


Figure 12. Variation of Logarithmic Decrement with Temperature in an Evacuated Environment, Test No. 2.



and also in Fig. 17, the saturation curve.

In examining the damping characteristics as a function of temperature, it was found that the logarithmic decrement decreased somewhat with increasing temperature and then increased rapidly with further increase above 400 F. These results compared with those presented by Contractor and Thompson (10) and were in agreement with a similar study conducted by Anderson (17) for the lower temperature range.

Data were not available on the damping characteristics for higher temperatures; however, as expected, the logarithmic decrement continued to increase very rapidly above 500 F. It should be noted again that the temperatures observed were those just outside the support and that a gradient existed along the beam, the free end being at a higher temperature. The temperature differences between the two ends are shown in Fig. 13.

The plot of logarithmic decrement versus temperature also shows that as the temperature increased, the effect of the magnetic field or magnetostrictive damping decreased. This effect became negligible at about 550 F as the two curves approached each other. This indicates that the beam had reached the Curie temperature, the point at which a ferromagnetic material loses its magnetic properties. The Curie point for a steel of this type is 670 F which seemed to be reasonable considering the gradient which existed along the beam.

Included in this study is a plot showing how the beam frequency changed with temperature. The frequency change was almost linear in the range observed, as shown in Fig. 14. The decrease can be attributed to two factors, namely, 1) change in the damping capacity which changes the damped natural frequency and 2) the change in the modulus of elasticity of the material with temperature change.



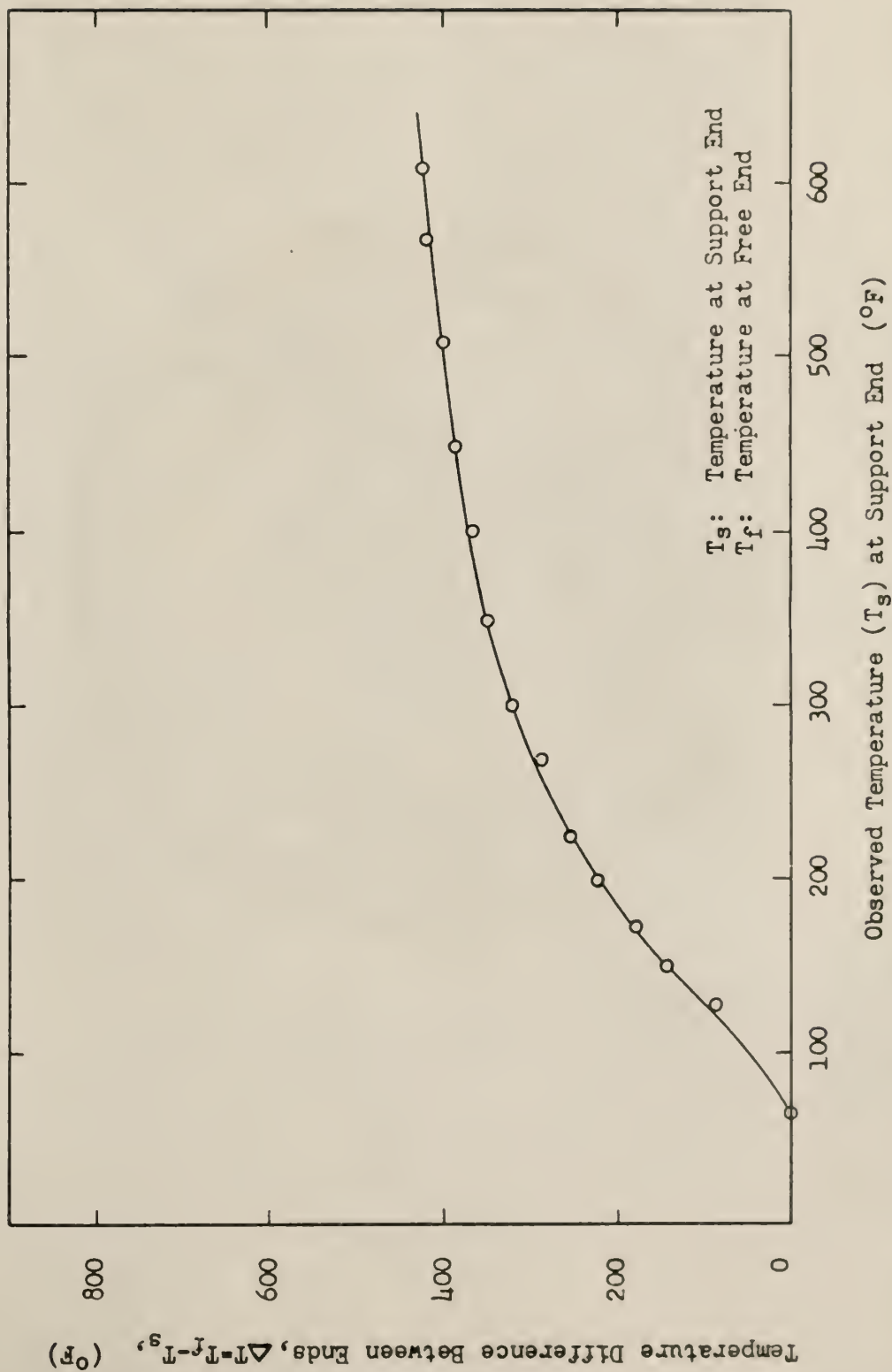


Figure 13. Variation in Temperature Between the Ends with Observed Temperature at Support End in an Evacuated Environment.

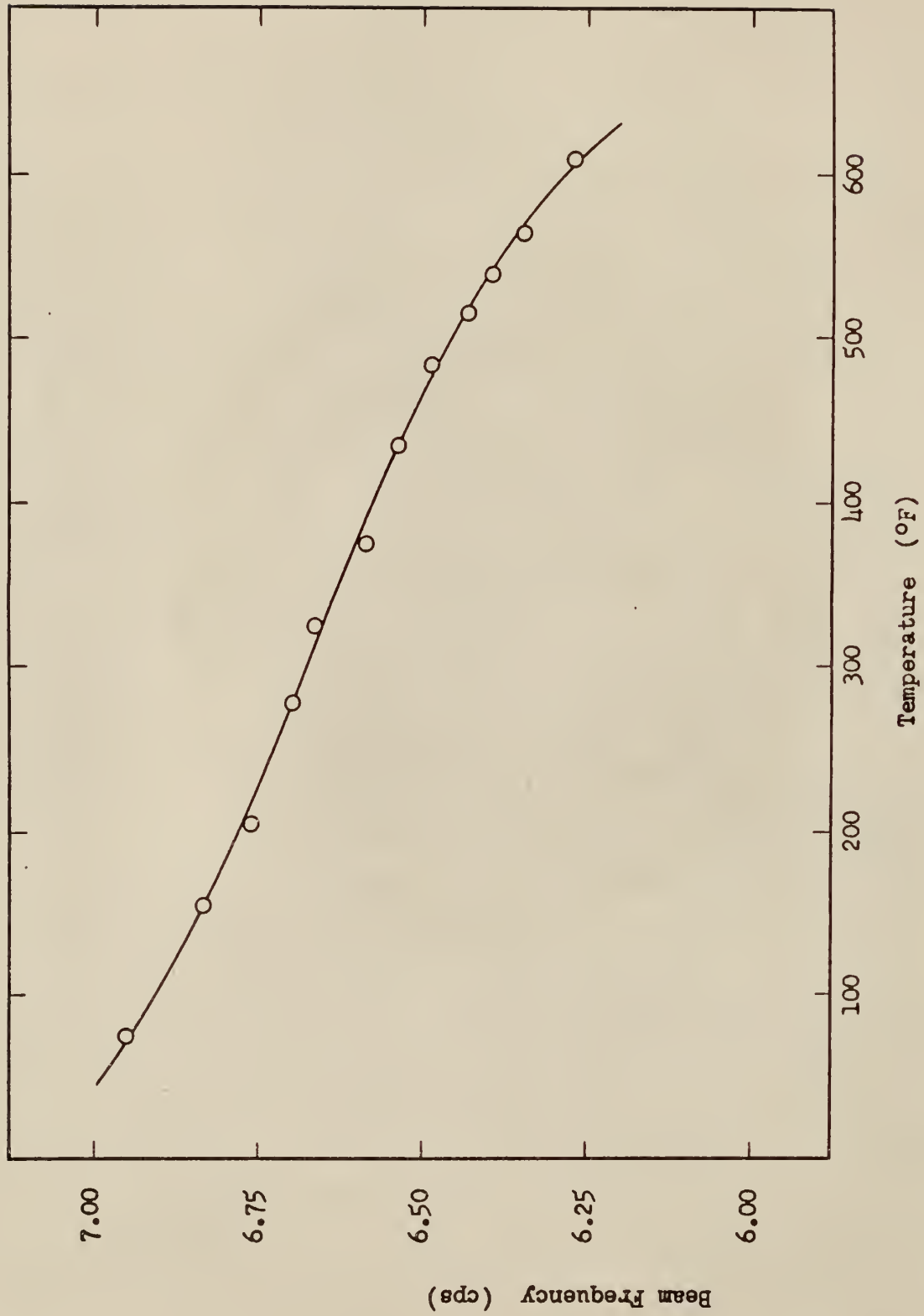


Figure 14. Variation of Beam Frequency with Temperature, Tests No. 1 and 2.

## PART VII

### CONCLUSIONS AND RECOMMENDATIONS

It is concluded from these test results that, for the specimen tested (1020 hot rolled steel), the effect of a magnetic field or magnetostrictive damping is an easily measurable and significant portion of the total internal damping. Since the viscous and pressure drag effects of air were negligible, the remaining small portion of the internal damping can be attributed to those sources mentioned earlier: plastic flow, thermoelastic effect, and atomic diffusion. It was believed that since the effects of the above three sources is by theory very small for the conditions tested, a significant part of the remaining portion was due to external damping in the support. Therefore, it is estimated that magnetostrictive damping may account for as much as 75% of the total internal damping in the lower temperature range.

With regard to the effect of temperature on damping, it is concluded that the damping is lowered slightly with an increase in temperature above 80 F and remains relatively constant up to about 350-400 F at which time the damping increases sharply. This sharp increase, broadly speaking, appears to be due to the sudden development of a "plastic" condition in the material.

It would be desirable to repeat these tests for several different ferromagnetic as well as non-ferromagnetic materials at different stress levels in order to better compare materials for design purposes. Also it would be noteworthy to examine the same parameters in very low temperature ranges. Considering the limitations of the test apparatus used here, it would be

desirable to change the testing apparatus as listed below:

1. Consider a free-free vibrating member so that energy loss to the supports in the form of heat and damping can be reduced.
2. Use a radiation furnace within the vacuum chamber to obtain constant temperatures throughout the specimen and eliminate the necessity for a "U" shaped beam.
3. Measure amplitudes of deflections with the use of an optical-electronic transducer coupled with an oscillograph to eliminate any lead wires being attached to the vibrating beam.

A recommendation is also made to further investigate the effects of shielding and altering the damping properties with the use of non-ferromagnetic shielding around the vibrating member. This is made in view of the results obtained while using the aluminum heat shield within the field coil. Reference is made to Fig. 8 of this report.

## REFERENCES

1. Demer, L. J. "Bibliography of the Material Damping Field." WADC Technical Report 56-180, June, 1956.
2. Thompson, Sir William, and Lord Kelvin. "On the Elasticity of Viscosity of Metals." Proceedings of the Royal Society of London, May 18, 1865.
3. Hopkinson, B., and G. Williams. "The Elastic Hysteresis of Steel." Proceedings of the Royal Society of London, 1912, 87:502-511.
4. Föppl, O. "The Practical Importance of Damping Capacity of Metals Especially Steels." Journal of the Iron and Steel Industries, 1936, 134:393-455.
5. Kimball, A. L. "Internal Friction Theory of Shaft Whirling." Physical Review, 1923, 21 (2):703.
6. Kimball, A. L., and D. E. Lovell. "Internal Friction in Solids." Physical Review, 1927, 30 (2):948-959.
7. Cochardt, A. W. "The Origin of Damping in High-Strength Ferromagnetic Alloys." ASME Transactions, 1953, 75:196,574.
8. Seitz, F., The Physics of Metals. New York: McGraw-Hill Book Co., 1943.
9. Robertson, J. M., and A. J. Yorgiadis. "Internal Friction in Engineering Materials." ASME Transactions, 1946, 68:2-173-181.
10. Contractor, G. P., and F. C. Thompson. "The Damping Capacity of Steel and Its Measurement." Journal of Iron and Steel Institute, 1940, 141: 157-183.
11. Plunkett, R. "Measurement of Damping." ASME Applied Mechanics Division, Shock and Vibration Committee. Structural Damping, edited by J. E. Ruzicha, Papers Presented at Colloquium at Atlantic City, 1959.
12. Crede, C. E. Vibration and Shock Isolation, New York: John Wiley, 1956.
13. Jacobsen, L. S. "Steady Forced Vibration as Influenced by Damping." ASME Transactions, 1930, 52:169.
14. Lytton, J. L., J. A. Hren, K. T. Kamber, and O. D. Sherby. "Apparatus for the Determination of Dynamic Young's Modulus and Internal Friction in Vacuum at Temperatures from 25 C to 1200 C." Brit. Journal of Applied Physics, 1964.



15. Kimball, A. L. Vibration Prevention in Engineering, New York: John Wiley, 1932, p. 116.
16. Parker, E. R. "The Influence of Magnetic Fields On Damping Capacity." Transactions of the A. S. M., 1940, 28:661-668.
17. Anderson, N. R. "Magnetostrictive Damping of Two Ferromagnetic Alloys at Elevated Temperatures." A Master's Report, Kansas State University, 1966.
18. McWithey, R. R. and R. J. Hayduk. "Damping Characteristics of Built-Up Cantilever Beams in a Vacuum Environment." NASA, TND-3065.
19. Dow, J. P. "Pressure and Frequency Effects on the Damping of a Cantilever Beam in a Magnetic Field." A Master's Report, Kansas State University, 1967.

## APPENDIX

## APPENDIX A

### EQUIPMENT LIST

The following is a list of the experimental equipment and measuring instruments used during this experiment. Numbers refer to the notation in Figs. 4, 5, 6, and 7.

1. Vacuum Chamber
2. Vacuum Pump, Welch Scientific Company, model no. 1399
3. Mercury Manometer, King Engineering Corp., model no. BUS-36
4. Pirani Gauge, Consolidated Electrodynamics Corp., type GP-110, 0 to 2000 microns full scale
5. Deflecting Mechanism
6. Magnetic Field Coil
7. Radiation Heat Shield and Cooling Coil
8. Beam Specimen
9. Cantilever Beam Support
10. Welder (AC Power Supply), Lincoln Company, model TM-500/500
11. Sanborn Recorder, Sanborn Company, model no. 127 T  
Sanborn Strain Gage Amplifier, Sanborn Company, model no. 140 B
12. DC Power Supply, Consolidated Electrodynamics Corp., type no. B-131, variable range
13. Millivolt Potentiometer, Leeds and Northrup Co., model 8696
14. DC Ammeter, Weston Co., model 901, 0 to 10 amp. range
15. AC Ammeter (clamp on), Bruno-New York Industries, 0 to 600 amp range
16. Calibration Weights
17. DC Power Supply, Eico, model no. 1064, variable range

## APPENDIX B

### CALIBRATION PROCEDURE

In order to find a relation between recorder pen deflection and the maximum stress in the beam, it was necessary to first calculate stress as a function of a concentrated load at the end. For a simply supported cantilever beam with a concentrated load, the maximum bending stress is given by

$$\sigma = Mc/I \quad .$$

In this case of a double rod, I is given by

$$I = 2(\pi R^4/4) = \pi D^4/32$$

and  $c = D/2$ . The maximum stress is hence

$$\sigma = 16 Pl/\pi D^3 \quad .$$

For the specimen tested, with a diameter of 0.313 inches and a length of 34.50 inches, the stress-load relationship was found to be

$$\sigma = 5750 P$$

where P is the concentrated load in pounds.

The beam was then loaded progressively from no-load to 1.0 pound while recording the stylus deflection. This was done at various temperatures to determine the sensitivity at each temperature. A direct relationship was hence obtained between the maximum stress and pen deflection for each temperature. These linear relationships are shown in Fig. 15. These curves were necessary in order to analyze all data at a constant stress level of 1500 psi.

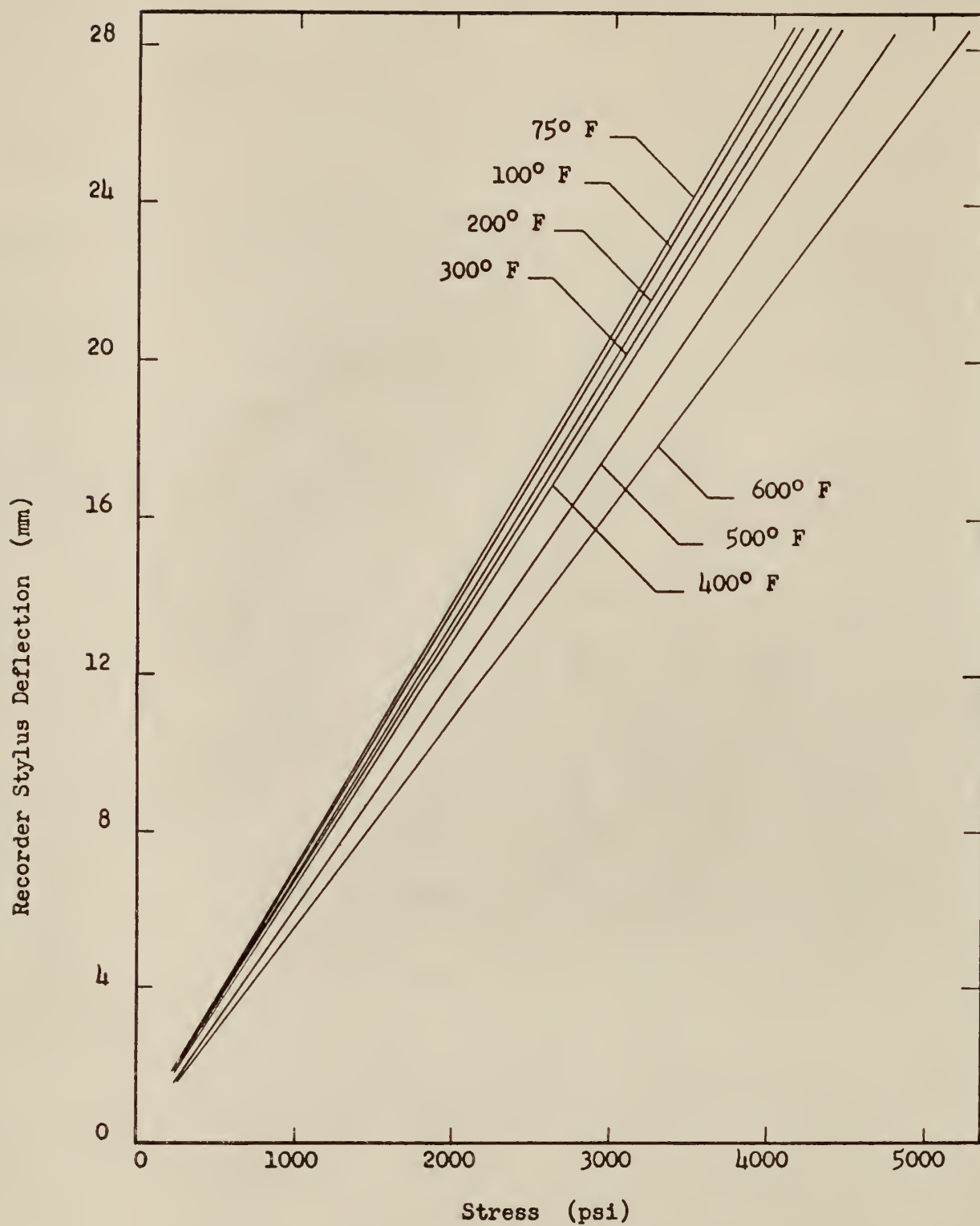


Figure 15. Variation of Stylus Deflection with Maximum Stress at Various Temperatures.



## APPENDIX C

### DETERMINATION OF EFFECTS OF AIR PRESSURE UPON DAMPING

Since all the tests were conducted in an evacuated environment, an attempt has been made to show that the viscous effect and the pressure drag of air has been eliminated or that it can be considered negligible. Fig. 16 shows the relationship between logarithmic decrement and the chamber pressure for the specimen tested.

McWithey and Hayduk (18) have indicated that the viscous-air drag becomes insignificant below 10,000 microns or 10 mm Hg. Similar studies reported by Dow (19) indicate also that the air drag becomes negligible below 4000 microns. All tests were conducted at a pressure of between 1000 and 2000 microns, well below that mentioned above.

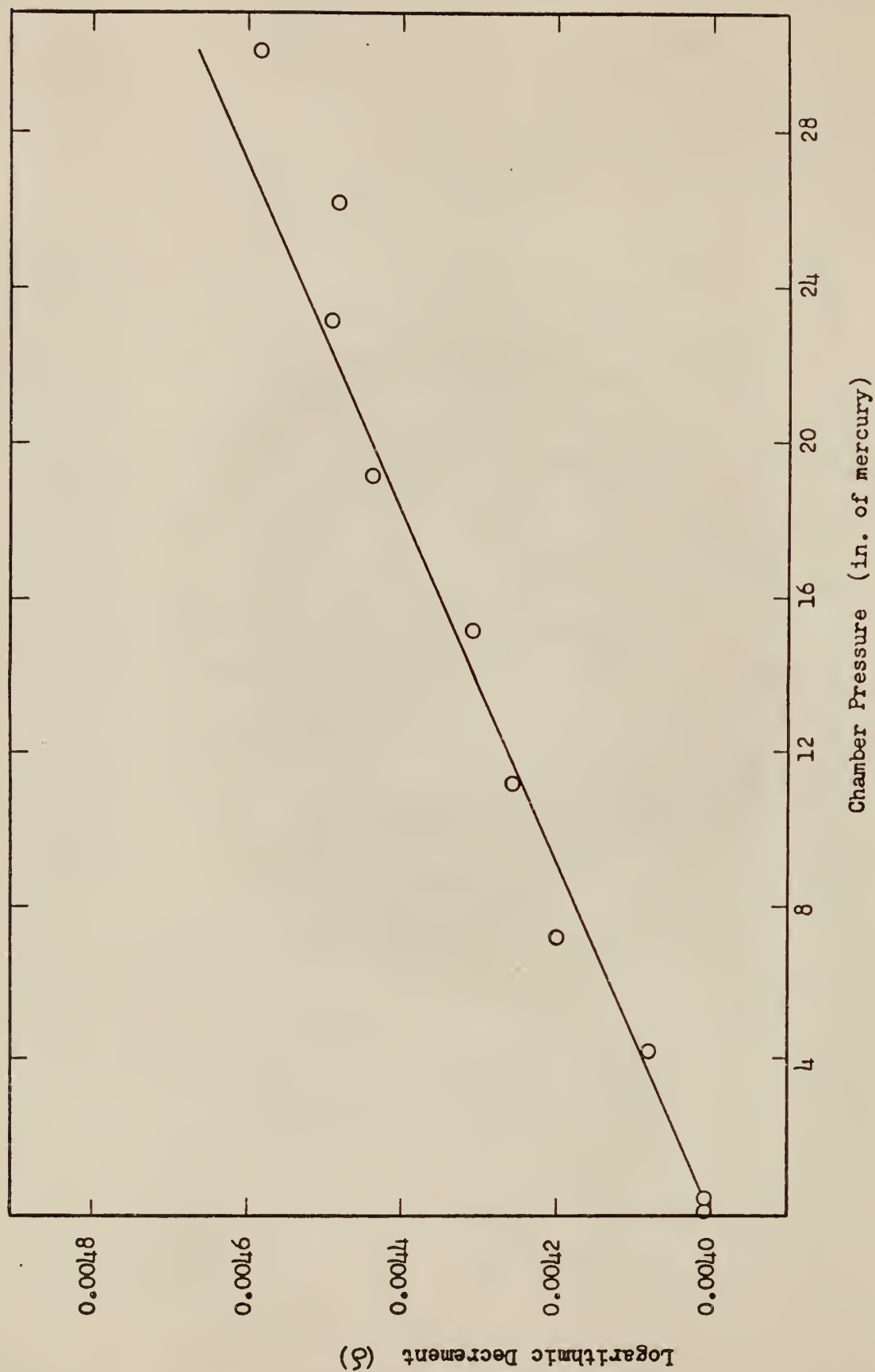


Figure 16. Variation of Logarithmic Decrement with Chamber Pressure.

## APPENDIX D

### DETERMINATION OF MAGNETIC SATURATION

Before performing any tests in the magnetic field, a saturation test was conducted to determine if the field current was sufficiently strong to eliminate magnetostrictive damping. To accomplish this, the logarithmic decrement was measured while varying the field current over the range, 0 to 4.2 amperes. This test was conducted in the evacuated chamber at room temperature.

A definite level of saturation was found for the specimen to be 2.5 amperes as shown in Fig. 17. A field current of 4.2 amperes was used in all tests to insure complete saturation.

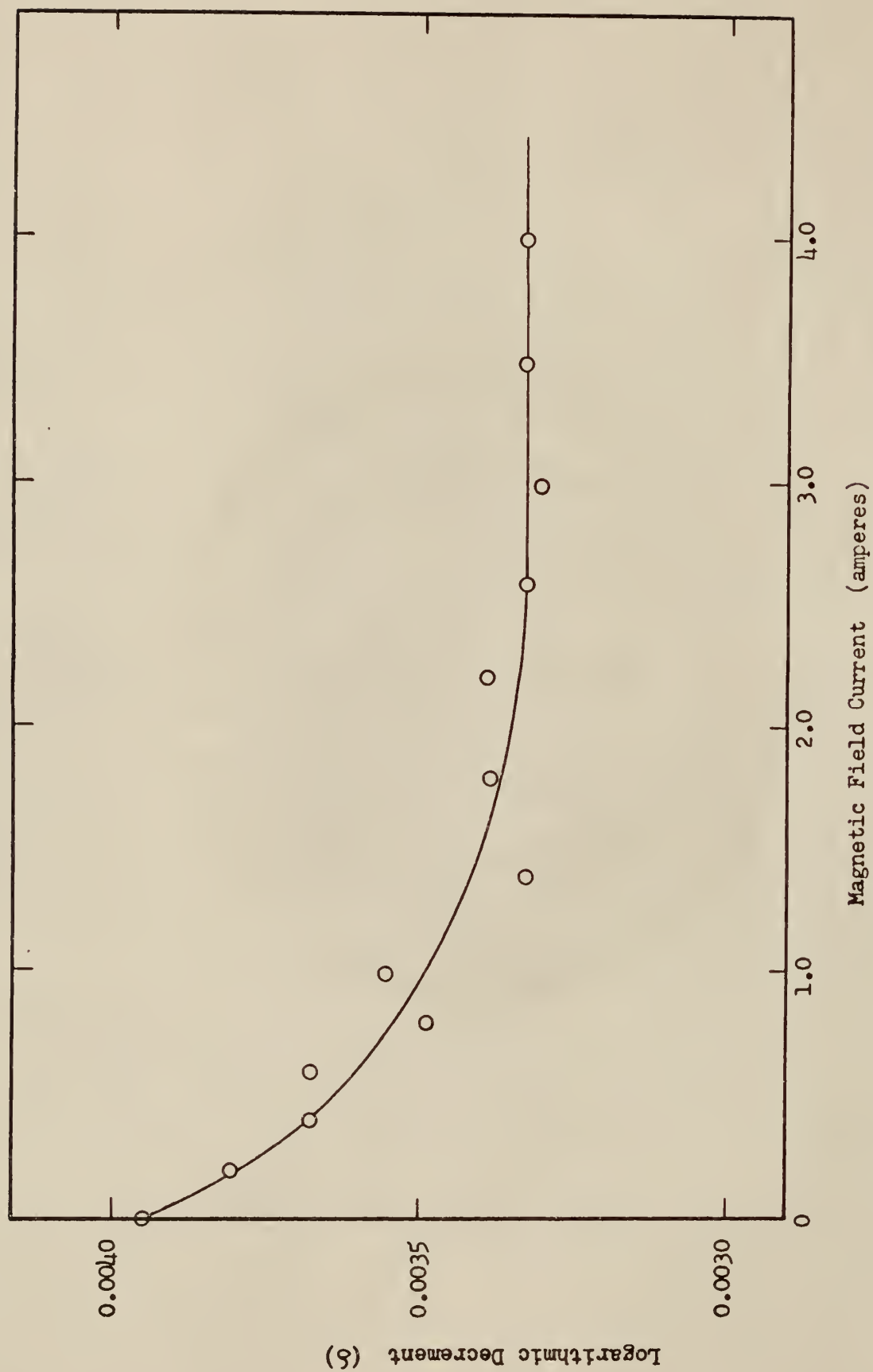
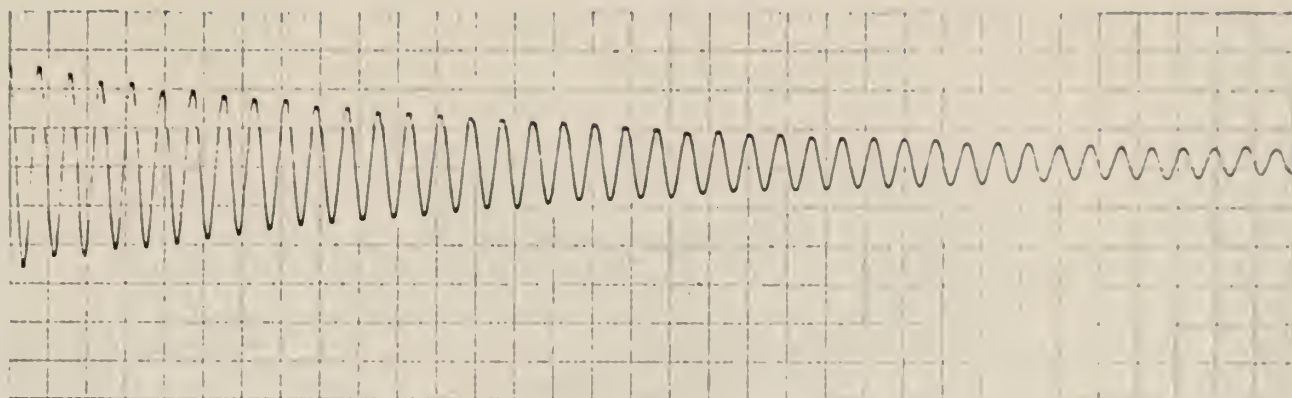


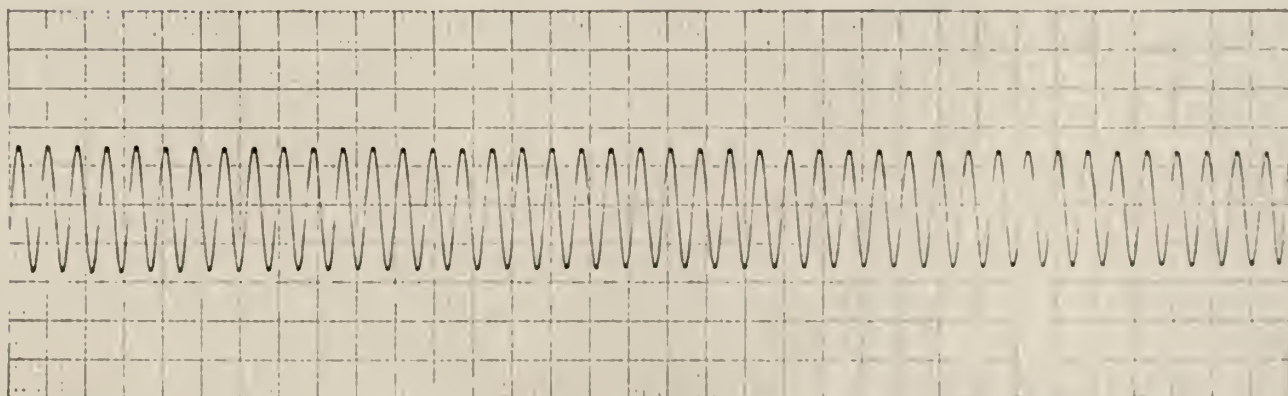
Figure 17. Variation of Logarithmic Decrement with Magnetic Field Current.

## APPENDIX E



Temperature: 610° F  
Pressure: 1000 microns  
Magnetic Field On: 4.2 amp.

Chart Speed: 25 mm/sec  
Sensitivity: 184 psi/chart line



Temperature: 435° F  
Pressure: 1000 microns  
Magnetic Field On: 4.2 amp.

Chart Speed: 25 mm/sec  
Sensitivity: 158 psi/chart line

Figure 18. Typical Recorder Traces



TABLE I

Typical Data — Test No. 1  
 Pressure: 1000 microns      Chart Speed: 25 mm/sec      Field Current: 4.2 amps.

Time (min.)	Temp. (°F)	$x_{n/2}$ (mm)	n (cycles)	Field		No Field		Heating Current
				$x_o$ (mm)	$x_n$ (mm)	$x_o$ (mm)	$x_n$ (mm)	
0	78	21.0	100	24.8	17.7	25.5	17.6	53
17	155	20.6	100	23.2	18.8	25.8	16.8	65
36	207	20.4	100	22.9	18.6	20.3	16.7	80
55	278	20.1	100	21.9	18.1	23.7	17.0	90
68	324	19.8	100	22.0	18.0	22.6	17.1	100
85	376	19.6	100	22.1	17.7	22.2	17.0	110
100	436	19.0	100	21.4	16.9	22.0	16.7	120
110	483	18.3	100	22.8	15.0	23.4	15.8	125
120	516	18.0	100	26.9	12.3	28.0	11.8	128
126	542	17.2	50	25.1	12.3	26.0	11.4	130
130	565	17.0	20	22.0	13.0	22.0	13.0	132
134	610	16.4	10	21.8	12.6	21.8	12.6	137

Note:  $x_{n/2}$  is the peak to peak amplitude corresponding to 1500 psi from Fig. 15, Appendix B. All  $x$ 's are peak to peak amplitudes.

## APPENDIX F

### DERIVATION OF LOGARITHMIC DECREMENT

In deriving the equation for the logarithmic decrement, it is assumed that the system is vibrating in a single mode shape. The system is also assumed to be viscously damped; that is, one in which the energy loss per cycle is proportional to the square of the amplitude or stress. For the simple system, the response will give a damped wave similar in general appearance to Fig. 19 from which we may compute the system damping.

To develop the method, assume that the system is shock excited by displacing the mass some distance  $x_0$  and then releasing it. It is reasonable to assume the theoretical wave equation as the solution

$$x = e^{-\zeta \omega_n t} [A \sin \omega_d t + B \cos \omega_d t] \quad (1)$$

where  $\omega_n$  = undamped natural frequency, rad./sec

$\zeta = C/2m \omega_n$ , damping ratio

$\omega_d = \omega_n \sqrt{1 - \zeta^2}$ , damped natural frequency, rad./sec

The boundary conditions are forced to be

$$\begin{aligned} t = 0 & \quad , \quad x = x_0 \quad ; \\ t = 0 & \quad , \quad \frac{dx}{dt} = 0 \quad . \end{aligned}$$

Applying these boundary conditions gives

$$B = x_0 \quad ,$$

$$A = \frac{x_0 \zeta \omega_n}{\omega_d} = \frac{x_0 \zeta}{\sqrt{1 - \zeta^2}} \quad .$$

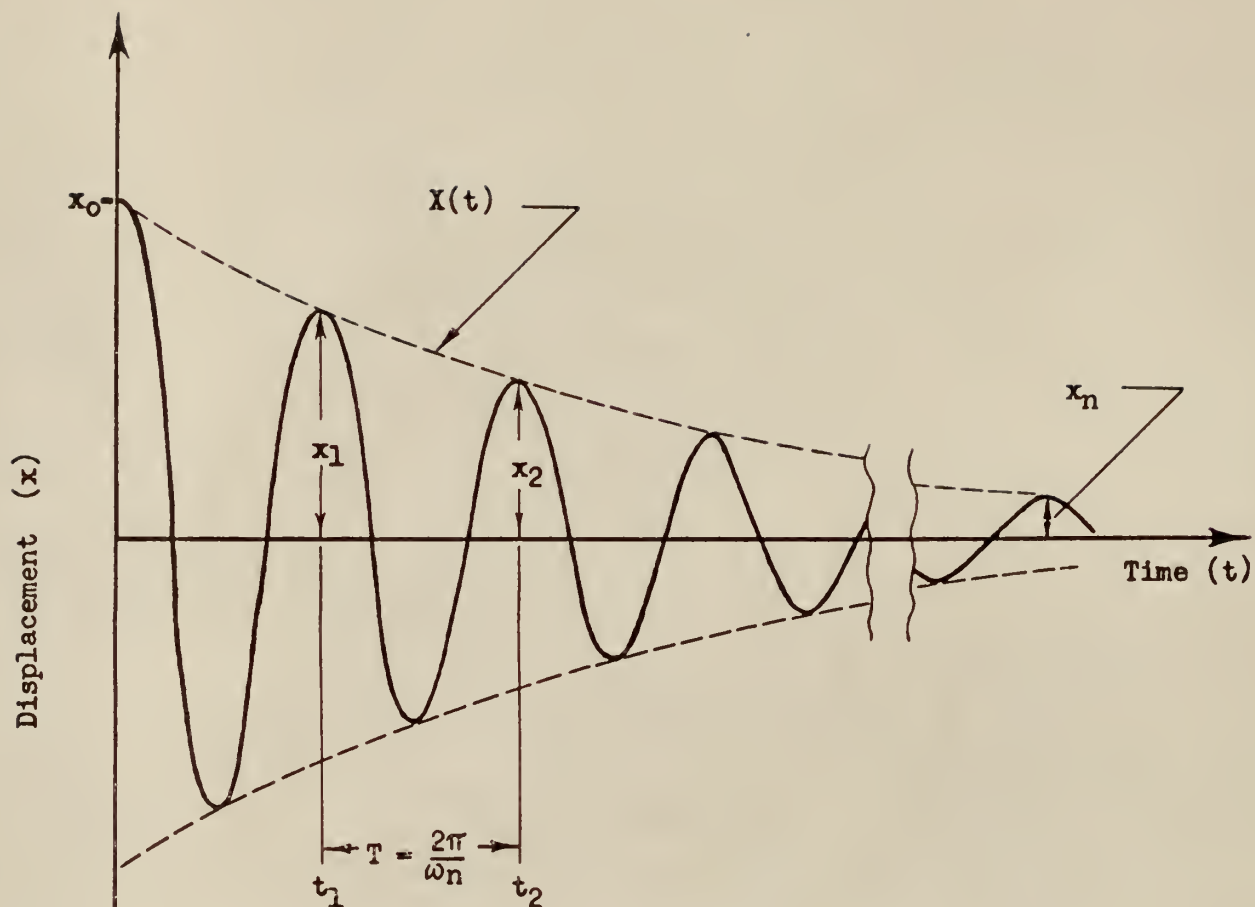


Figure 19. Free vibration with damping: initial conditions  $x(0) = x_0$  and  $\dot{x}(0) = 0$ .

Consequently, the displacement response is

$$x = \frac{x_0 e^{-\zeta \omega_n t}}{\sqrt{1 - \zeta^2}} \left[ \sqrt{1 - \zeta^2} \cos \omega_d t + \zeta \sin \omega_d t \right] \quad (2)$$

Applying certain trigonometric identities and simplifying, the displacement is reduced to the form

$$x = \frac{x_0 e^{-\zeta \omega_n t}}{\sqrt{1 - \zeta^2}} \cos(\omega_d t - \phi) \quad (3)$$

$$\text{where } \phi = \tan^{-1} \frac{\zeta}{\sqrt{1 - \zeta^2}} .$$

The equation of the envelope of this displacement response is the first part of Eq. (3)

$$X(t) = \frac{x_0 e^{-\zeta \omega_n t}}{\sqrt{1 - \zeta^2}} \quad (4)$$

and this envelope will touch the response curve very close to the points at which the argument of Eq. (3),  $(\omega_d t - \phi)$ , is equal to  $360^\circ$ ,  $720^\circ$ , etc., as indicated in Fig. 19. Thus Eq. (4) is very nearly a correct expression for the maximum value of  $x$ , provided the correct time  $t$  is used.

To eliminate  $t$ , let  $t_1$  be the time at one peak of the response curve and note that the next peak is one period and hence  $T$  seconds later. Since

$$T = \frac{1}{f_n} = \frac{2\pi}{\omega_d}$$

the time at this next peak is given by

$$t_2 = t_1 + \frac{2\pi}{\omega_d} .$$

Using these values of time in conjunction with Eq. (4) gives the ratio of

the peaks as

$$\frac{x_1}{x_2} = \frac{e^{-\zeta \omega_n t_1}}{e^{-\zeta \omega_n t_2}} = e^{\zeta \omega_n (2\pi/\omega_d)} = e^{2\pi\zeta/\sqrt{1-\zeta^2}} .$$

The natural logarithm of this ratio of successive peaks in the decay curve is called the logarithmic decrement, and is

$$\delta = \ln \frac{x_1}{x_2} = \frac{2\pi\zeta}{\sqrt{1-\zeta^2}} .$$

Since the rate of decay of the oscillatory motion is independent of the initial conditions imposed on the system, the logarithmic decrement must be independent of initial conditions. Furthermore, any two points on the curve (Fig. 19) one period apart may serve to evaluate the logarithmic decrement,

$$\frac{x_1}{x_2} = \frac{x_2}{x_3} = \dots = \frac{x_{n-2}}{x_{n-1}} = \frac{x_{n-1}}{x_n} = e^{\delta} .$$

Hence

$$\frac{x_1}{x_n} = \frac{x_1}{x_2} \cdot \frac{x_2}{x_3} \dots \frac{x_{n-1}}{x_n} = e^{n\delta} ,$$

$$\ln \frac{x_1}{x_n} = n\delta ,$$

$$\delta = \frac{1}{n} \ln \frac{x_1}{x_n} .$$

Therefore the logarithmic decrement may be evaluated from two known amplitudes  $n$  cycles apart.



#### ACKNOWLEDGEMENTS

The author wishes to express his appreciation to Dr. H. S. Walker of the Department of Mechanical Engineering, Kansas State University, for his excellent guidance and technical direction throughout the course of this work as his advisor.

The author is also grateful to Dr. R. G. Nevins, Head, Department of Mechanical Engineering, Kansas State University, for his confidence and financial assistance.

VITA

Donald L. Carter

Candidate for the Degree of  
Master of Science

Report: THE INFLUENCE OF TEMPERATURE AND MAGNETIC FIELDS ON DAMPING CAPACITY  
IN AN EVACUATED ENVIRONMENT

Major Field: Mechanical Engineering

Biographical:

Personal Data: Born at Maryville, Missouri, March 10, 1943, the son of  
Harry C. and Velma I. Carter.

Education: Graduated from North Andrew High School, Rosendale, Missouri  
in 1961: received the Bachelor of Science degree from the University  
of Missouri at Rolla, with a major in Mechanical Engineering, in  
June, 1965; completed requirements for the Master of Science degree  
in June, 1967.

Professional experience: Employed as a summer engineer for Collins Radio  
Company during summer, 1964; employed as an engineering trainee for  
Deere and Company during summer, 1965; taught in the Mechanical Engi-  
neering Department at Kansas State University as a part-time instruc-  
tor during fall semester, 1966.

THE INFLUENCE OF TEMPERATURE AND MAGNETIC FIELDS  
ON DAMPING CAPACITY IN AN  
EVACUATED ENVIRONMENT

by

DONALD LAVERNE CARTER

B. S., University of Missouri at Rolla, 1965

---

AN ABSTRACT OF A MASTER'S REPORT

submitted in partial fulfillment of the

requirements for the degree

MASTER OF SCIENCE

Department of Mechanical Engineering

KANSAS STATE UNIVERSITY  
Manhattan, Kansas

1967

Name: Donald L. Carter

Date of Degree: August 4, 1967

Institution: Kansas State University

Location: Manhattan, Kansas

Title of Study: THE ENFLUENCE OF TEMPERATURE AND MAGNETIC FIELDS ON DAMPING  
CAPACITY IN AN EVACUATED ENVIRONMENT

Pages in Study: 54

Candidate for Degree of Master of Science

Major Field: Mechanical Engineering

Scope and Method of Study: Internal friction or damping capacity is that property of a solid material which results in energy absorption when the material is stressed cyclically. This material property is an important design parameter to consider in the design of certain structures. In analyzing the internal damping, it is necessary to examine what factors affect damping and how these variables enfluence damping over certain ranges. This study was concerned with the enfluence of magnetic fields and high temperatures on the damping of a low carbon steel in an evacuated environment.

The study was carried out by observing the decay rate of a cantilever beam heated electrically within a vacuum chamber. The beam was given a initial deflection and released. The amplitude of the free vibration was measured with a resistance strain gage bonded to the beam and the output permanently recorded on paper. The enfluence of a magnetic field was observed over a temperature range of 75-610° F.

Findings and Conclusions: The results of these tests indicated that the damping due to a magnetic field or magnetostrictive damping accounts for a significant portion of the total internal damping over a temperature range of 75-400° F. This effect decreased to zero as the temperature increased further toward the Curie point of the material.

With regard to temperature effects upon damping, it was found that the damping is lowered slightly above 80° F and remains relatively constant up to about 350-400° F at which time it increases. Above this temperature the damping increases sharply, the material appearing to reach a "plastic" condition.

MAJOR PROFESSOR'S APPROVAL

Hugh L. Walker



